Supporting Information

Matt et al. 10.1073/pnas.1204073109

SI Methods

Construction of Mutant Strains. The single ribosomal RNA (rRNA) allelic *rpsL*$^+$ *Mycobacterium smegmatis* ΔrrnB (SZ380) was obtained by unmarked deletion mutagenesis and was used for all genetic constructions (1). Genetic manipulations of the single chromosomal rRNA operon were done as described previously (2). Selective plating and RecA-mediated homologous recombination were used for gene replacement. Successful gene replacement was controlled by sequence analysis. For a list of plasmids and strains see Tables S6 and S7.

Bacterial Strains. Clinical isolates were obtained from the Diagnostic Department, Institute of Medical Microbiology, University of Zurich, Zurich. Recombinant *Escherichia coli* with defined aminoglycoside resistance determinants (Table S1) were kindly provided by P. Courvalin (Institut Pasteur, Paris, France).

Isolation and Purification of Ribosomes. Ribosomes were purified from bacterial cell pellets as described previously using sucrose gradient [10–40% (wt/vol)] centrifugation (3). Ribosome concentrations of 70S were determined by absorption measurements on the basis of 23 pmol ribosomes per A_{260} unit.

Cell-Free Luciferase Translation Assays. Purified 70S hybrid ribosomes were used in translation reactions of luciferase mRNA. Firefly and renilla luciferase mRNAs were produced using T7 RNA polymerase (Fermentas) in vitro on templates of modified plasmids pGL4.14 (firefly luciferase) and pGL4.75 (renilla luciferase) (both from Promega). In these plasmids the mammalian promoter driving transcription of luciferases was replaced by the T7 bacteriophage promoter. A typical translation reaction with a total volume of 30 μL contained 0.25 μM 70S ribosomes, 4 μg firefly luciferase (F-luc) mRNA, 0.4 μg Renilla luciferase (R-luc) mRNA, 40% (vol/vol) of *M. smegmatis* S100 extract, 200 μM amino acid mixture, 24 units of RiboLock (Fermentas), 0.4 mg/mL of total *E. coli* tRNA, and 12 μL of commercial S30 Premix without amino acids (Promega). After the addition of serially diluted aminoglycosides, the reaction mixture was incubated at 37 °C for 35 min, stopped on ice, and assayed for F-luc and R-luc activities using the Dual-Luciferase Reporter Assay System (Promega). Luminescence was measured using a luminometer (FLx800; Bio-Tek Instruments). R-luc activity was used as an internal standard.

Misreading was assessed in a gain-of-function assay as described (4). We introduced Arg245 (CGC near-cognate and AGA noncognate codon) into the F-luc protein to replace residue His245 (CAC codon). Arg245 F-luc mRNA and wild-type F-luc mRNA were used in in vitro translation reactions; in addition, R-luc mRNA was used as internal control. We quantified misreading by calculating mutant firefly/renilla luciferase activity compared with wild-type firefly/renilla luciferase activity.

Mitochondrial *in Organello* Translation. Mitochondria were isolated from HEK293 cells as described (5). In brief, HEK293 cells were collected from a 90% confluent 10-cm plate, washed with 1× PBS, and resuspended in 1 mL of extraction buffer [20 mM Hepes-KOH (pH 7.5), 0.25 M sucrose, 10 mM KCl, 1.5 mM $MgCl_2$, 1 mM EDTA, 1 mM EGTA, 1 mM DTT]. Cells were broken by passing five times through a syringe needle (0.45 × 12 mm) and were centrifuged for 5 min at 800 × *g*; then supernatant was transferred to a new Eppendorf tube. The pellet was resuspended in 1 mL of extraction buffer, passed through a syringe needle (0.45 × 12 mm), and centrifuged for 5 min at 800 × *g*. The supernatant was collected, combined with the previous supernatant, and centrifuged for 15 min at 10,000 × *g*. The resulting pellet was used as the mitochondria-enriched fraction.

Mitochondrial in organello translation was done as described, with slight modifications (6–8). In brief, the mitochondria-enriched pellet was resuspended in 1 mL of mitochondria reaction buffer containing 20 mM Tris·HCl (pH 7.2), 90 mM KCl, 4 mM $MgSO_4$, 1.5 mM KH_2PO_4, 20 mM glutamate, 0.5 mM malate, 14 mM sucrose, 44 mM sorbitol, 1 μM methionine, 2 mM ADP, 0.1 mM amino acids (methionine), 1 mg/mL BSA (fatty acids free), 0.1 mg/mL cycloheximide. Fifteen microliters of S35-methionine [370 MBq (10 mCi)/mL, specific activity 37 TBq (1,000 Ci)/mmol] (KSM-01; Hartmann Analytic) were added, the suspension was split into 54-μL aliquots, and drugs were added to a final reaction volume of 60 μL (compounds were dissolved in H_2O with pH adjusted to 7.5 using 5 M KOH). Reaction mixtures were incubated for 2 h at 30 °C with shaking. After incubation the reaction mixtures were centrifuged for 5 min at 15,000 × *g*, and the supernatants were discarded. The pellets were washed with cold washing buffer containing 10 mM Tris·HCl (pH 7.4), 320 mM sucrose, 1 mM EDTA, were centrifuged for 5 min at 15,000 × *g*, and were resuspended in 10 μL of H_2O. SDS loading buffer was added, and the samples were resolved by 18% (wt/vol) SDS/PAGE. The gel was fixed, dried, and exposed on a phosphoimager screen. Translation was quantified using Aida Image Analyzer v. 3.52 program (Fuji) by scanning COX1 protein expression. The IC_{50} values represent the drug concentration that inhibits COX1 synthesis by 50%.

Aminoglycoside-Induced Inhibition of Protein Synthesis in Rabbit Reticulocyte Lysate and in HEK293 Cells. Rabbit reticulocyte lysate (RRL) (Promega) was used for in vitro translation. A standard 15-μL reaction contained 10 μL RRL, 2 μg of in vitro-transcribed reporter mRNA, 200 μM amino acid mixture, 12 U RNasin (Fermentas), and serially diluted aminoglycosides. The reaction mixture was incubated at 37 °C for 35 min. After incubation, luciferase assay substrate (Promega) was added (75 μL), and luciferase activities were determined using a luminescence microplate reader.

HEK293 cells were grown to 80% confluency at 37 °C in DMEM supplemented with 10% FBS (vol/vol) (Invitrogen) and subsequently were transfected using TurboFect transfection reagent (Fermentas) and pRM hRluc-hFluc according to the manufacturer's instructions. After transfection cells were incubated for 24 h. Medium was replaced by F10 (Invitrogen) without FBS. Serially diluted aminoglycoside antibiotics were added together with saponin (7.5 μg/mL), and cells were incubated for another 24 h. Cells were lysed, and luciferase activities were determined.

Vector pRM hRluc-hFluc was constructed on the basis of vectors pGL4.14 and pGL4.75 (Promega). After digestion of pGL4.14 with NheI/SalI the resulting 3.6-kb fragment (hFluc with SV40 polyA signal) was inserted into vector pGL4.75 digested with XbaI/SalI (hRluc under control of the CMV promoter). The resulting 7.6-kb transitional construct pRep-00 carries two separate genes, hRluc and hFluc. hRluc and hFluc were fused by a 27-nucleotide linker, encoding the nine-amino-acid polypeptide STCDQPFGF, using overlap PCR mutagenesis, resulting in vector pRM hRluc-hFluc.

Antibiotics. Gentamicin, kanamycin, tobramycin, and apramycin were obtained from Sigma. Aprosamine was synthesized using standard carbohydrate chemistry (9) and checked by NMR.

Minimal Inhibitory Concentrations. Minimal inhibitory concentrations (MIC) were determined by broth microdilution assays as described recently (2). Microtiter plates were incubated overnight for *E. coli, Pseudomonas aeruginosa*, and *Staphylococcus aureus* and for 72 h for *M. smegmatis, Mycobacterium abscessus, Mycobacterium massiliense*, and *Mycobacterium bolletii*. Drug susceptibility of *Mycobacterium tuberculosis, Mycobacterium avium-intracellulare* and *Mycobacterium kansasii* was assessed using the MGIT 960 instrumentation equipped with TBeXiST software (Becton-Dickinson) as described (10).

Crystal Structure Analysis. *Thermus thermophilus* 30S ribosomes were purified and crystallized as described previously (11). Crystals were soaked in the cryoprotectant solution [100 mM Mes-KOH (pH 6.5), 200 mM KCl, 75 mM NH_4Cl, 15 mM $MgCl_2$, and 26% (vol/vol) 2-Methyl-2,4-pentanediol (MPD)] that contains 100 μM of apramycin for 4 d before being flash-frozen. Crystals were prescreened, and the data set was collected at Swiss Light Source, Paul Scherrer Institute, Villigen, Switzerland. Data were integrated and scaled using XDS (12). A starting model consisting of the empty 30S ribosome [without anticodon-stem loop (ASL), mRNA, and ions] was used for initial refinement and phase calculation using Crystallography and NMR System (CNS) (13). The ASL and mRNA then were fitted into the unbiased difference (mF_o-DF_c) map, and the model was subjected to another round of refinement. Finally, five apramycin ligands were placed manually into an mF_o-DF_c map using COOT (14), which was refined to a resolution of 3.5 Å. One apramycin molecule was bound specifically to helix 44 at the decoding center. Another four secondary binding sites of apramycin were found at the platform and body of 16S rRNA, likely in an unspecific manner because of the high concentration of ligand soaking. The final refinement in Crystallography and NMR System had an Rwork/Rfree ratio of 19.4%/23.5%. Data and refinement statistics are reported in Table S8. Coordinates and structure factors have been deposited with the Protein Data Bank, accession code 4aqy.

Cochlear Explants. Drugs were screened for toxicity to hair cells in cochlear explants from CBA/J mice on postnatal day 3 (15). The dissected tissue was placed on a collagen-coated incubation dish in 1 mL of serum-free Basal Medium Eagle plus serum-free supplement (Invitrogen), 1% BSA, 2 mM glutamine, and 5 mg/mL glucose. The explants were incubated (37 °C, 5% CO_2) for 4 h, and an additional 1 mL of culture medium was added to submerse the explants. After 24 h the medium was exchanged for new medium containing the drugs, and the explants were incubated for 20 h. Cultures were fixed overnight in 4% (vol/vol) paraformaldehyde at 4 °C, and then were permeabilized for 30 min with 3% (vol/vol) Triton X-100 in PBS, washed three times with PBS, and blocked with 10% (vol/vol) goat serum for 30 min at room temperature. Following incubation at room temperature for 40 min with rhodamine-phalloidin (Molecular Probes), hair cell presence was determined by light microscopy of the phalloidin-stained stereociliary bundles and circumferential F-actin rings on the cuticular plate. Alternatively, the fixed cultures were reacted with a mouse monoclonal antibody to 3-nitrotyrosine (dilution 1:1,000) (Enzo Life Sciences) or a rabbit polyclonal antibody to myosin VIIa (dilution 1:200) (Proteus Biosciences) for 24 h at 4 °C. The primary antibodies were coupled with secondary antibodies (dilution 1:200) Alexa Fluor 488 (goat anti-mouse; green) or Alexa Fluor 546 (goat anti-rabbit; red) (Molecular Probes), respectively, for 2 h at room temperature. Nuclei were stained with Hoechst 33342 (1:1,000) for 45 min at room temperature.

In Vivo Ototoxicity. Pigmented male guinea pigs of initially about 200 g (Elm Hill Laboratories) had free access to water and food and were acclimated for 1 wk before experiments. Drugs were administered once daily s.c. for 16 d at dosages indicated in the figure legends; saline injections of the same volume served as controls. Auditory function was measured as auditory brainstem response at 12 kHz under anesthesia with an i.p. injection of 40 mg ketamine and 10 mg xylazine/kg body weight as described previously (16). For each animal the threshold was determined before the study and at 3 wk after drug treatment.

1. Hobbie SN, et al. (2006) A genetic model to investigate drug-target interactions at the ribosomal decoding site. *Biochimie* 88:1033–1043.
2. Pfister P, et al. (2005) Mutagenesis of 16S rRNA C1409-G1491 base-pair differentiates between 6′OH and 6′NH3+ aminoglycosides. *J Mol Biol* 346:467–475.
3. Bruell CM, et al. (2008) Conservation of bacterial protein synthesis machinery: Initiation and elongation in *Mycobacterium smegmatis*. *Biochemistry* 47:8828–8839.
4. Salas-Marco J, Bedwell DM (2005) Discrimination between defects in elongation fidelity and termination efficiency provides mechanistic insights into translational readthrough. *J Mol Biol* 348:801–815.
5. Pallotti F, Lenaz G (2001) Isolation and subfractionation of mitochondria from animal cells and tissue culture lines. *Methods Cell Biol* 65:1–35.
6. McKee EE, Grier BL, Thompson GS, McCourt JD (1990) Isolation and incubation conditions to study heart mitochondrial protein synthesis. *Am J Physiol* 258:E492–E502.
7. Fernández-Silva P, Acín-Pérez R, Fernández-Vizarra E, Pérez-Martos A, Enriquez JA (2007) In vivo and in organello analyses of mitochondrial translation. *Methods Cell Biol* 80:571–588.
8. McKee EE, Ferguson M, Bentley AT, Marks TA (2006) Inhibition of mammalian mitochondrial protein synthesis by oxazolidinones. *Antimicrob Agents Chemother* 50: 2042–2049.
9. O'Connor S, Lam LK, Jones ND, Chaney MO (1976) Apramycin, a unique aminocyclitol antibiotic. *J Org Chem* 41:2087–2092.
10. Springer B, Lucke K, Calligaris-Maibach R, Ritter C, Böttger EC (2009) Quantitative drug susceptibility testing of *Mycobacterium tuberculosis* by use of MGIT 960 and EpiCenter instrumentation. *J Clin Microbiol* 47:1773–1780.
11. Wimberly BT, et al. (2000) Structure of the 30S ribosomal subunit. *Nature* 407: 327–339.
12. Kabsch W (1993) Automatic processing of rotation diffraction data from crystals of initially unknown symmetry and cell constants. *J Appl Cryst* 26:795–800.
13. Brünger AT, et al. (1998) Crystallography & NMR system: A new software suite for macromolecular structure determination. *Acta Crystallogr D Biol Crystallogr* 54: 905–921.
14. Emsley P, Cowtan K (2004) Coot: Model-building tools for molecular graphics. *Acta Crystallogr D Biol Crystallogr* 60:2126–2132.
15. Chen F-Q, Schacht J, Sha SH (2009) Aminoglycoside-induced histone deacetylation and hair cell death in the mouse cochlea. *J Neurochem* 108:1226–1236.
16. Lautermann J, McLaren J, Schacht J (1995) Glutathione protection against gentamicin ototoxicity depends on nutritional status. *Hear Res* 86:15–24.

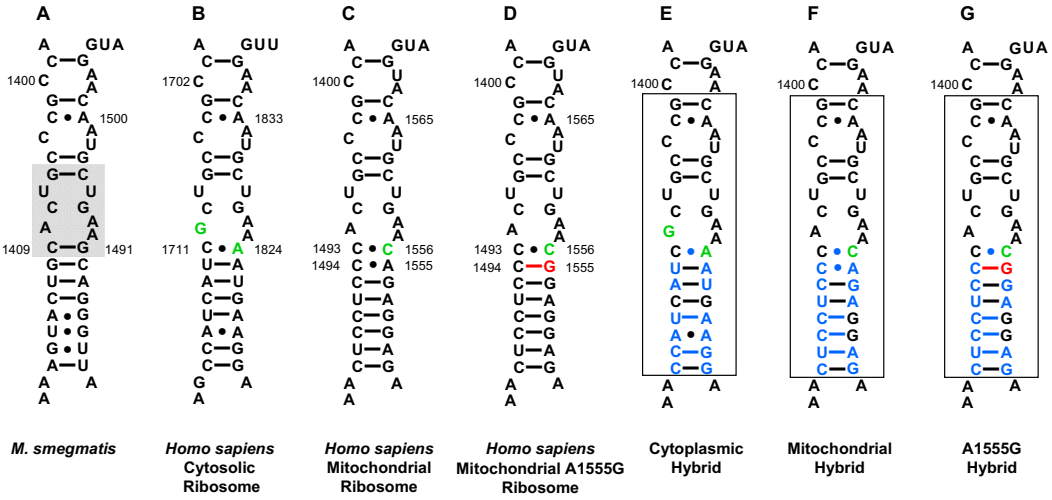

Fig. S1. Secondary-structure comparison of decoding-site rRNA sequences in the small ribosomal subunit. (*A*) Decoding region of 16S rRNA helix 44 in wild-type ribosomes of *M. smegmatis*; rRNA nucleotides are numbered according to the bacterial nomenclature, i.e., to homologous *E. coli* 16S rRNA positions. (*B*) Homologous 18S rRNA sequence in human ribosomes; rRNA residues are numbered according to the human cytoplasmic ribosome nomenclature. (*C*) Homologous 12S rRNA sequence in human mitochondrial ribosomes; rRNA residues are numbered according to the mitochondrial nomenclature. (*D*) Mitochondrial 12S rRNA sequence with mutation A1555G conferring hypersusceptibility to aminoglycoside antibiotics indicated in red. (*E*–*G*) Decoding site rRNA of human–bacterial hybrid ribosomes. The transplanted helix is boxed. Nucleotide positions depicted in blue represent residues that are specific for human rRNA. The aminoglycoside binding pocket (indicated in gray in *A*) is composed mainly of nucleotides of the A-site loop, in particular homologous *E. coli* positions G1405-C1496, U1406-U1495, C1407-G1494, A1408, A1492, A1493, and C1409-G1491. Phylogenetic differences in the drug-binding pocket impacting drug selectivity are shown in green.

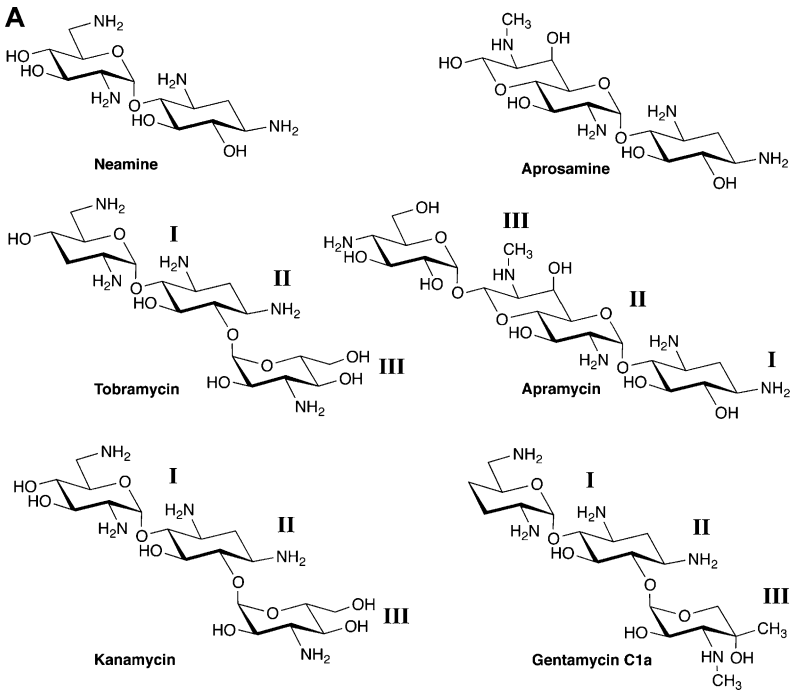

Fig. S2. (Continued)

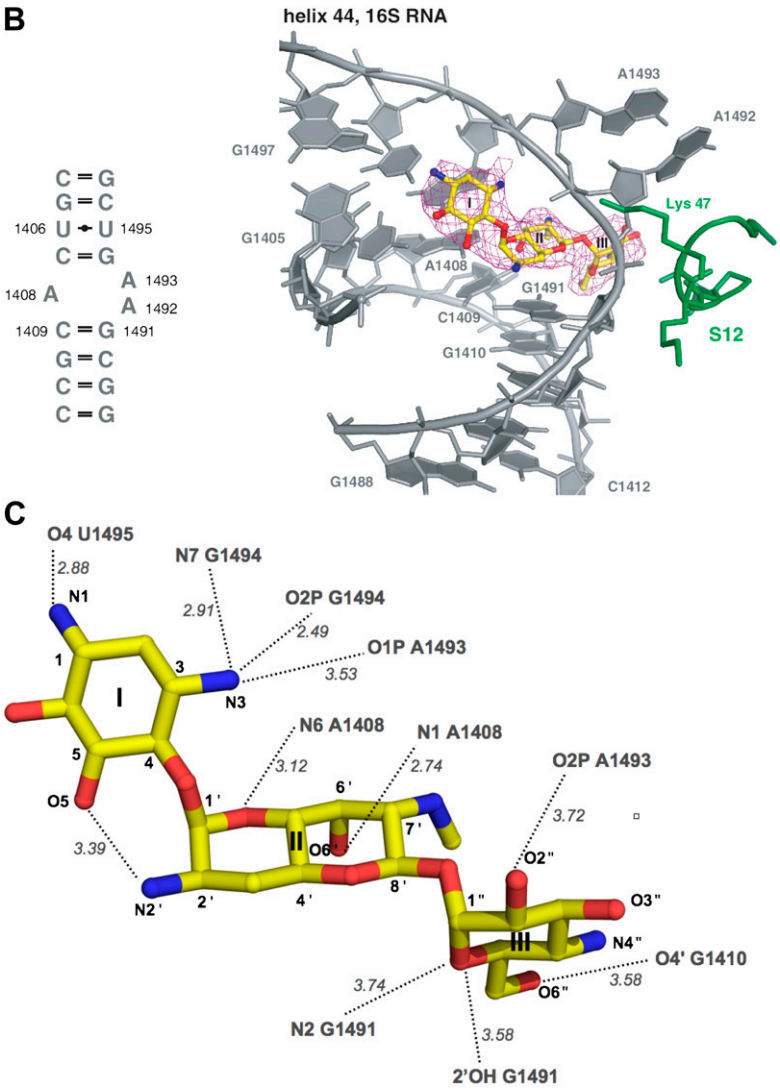

Fig. S2. (Continued)

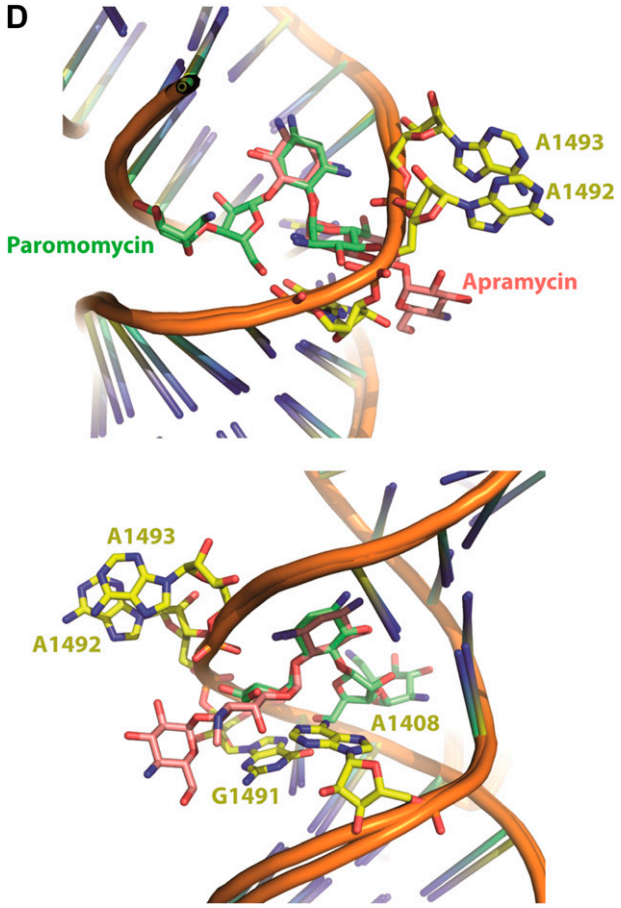

Fig. S2. Chemical structures of aminoglycoside antibiotics and crystal structure of apramycin in complex with the 30S subunit. (*A*) Chemical structures of aminoglycoside antibiotics. Note that the 2-deoxystreptamine moiety corresponds to ring I of apramycin and to ring II of the 4,6-disubstituted aminoglycosides. (*B*) Decoding site of 30S *Thermus thermophilus* subunit in complex with apramycin (*E. coli* numbering used throughout). Ribosomal protein S12 is shown in green. The unbiased difference (*mFo-DFc*) electron density map is displayed at 3.0 σ. (*C*) The interactions between apramycin and 16S rRNA nucleotides. Rings I, II, and III represent 2-deoxystreptamine, bicyclic ring, and ring III of apramycin, respectively. The hydrogen bonds are represented by gray dashed lines, with the distances stated in Ångstroms. (*D*) Two views of a superposition of apramycin (this work) and paromomycin bound to the 30S ribosomal subunit (Protein Data Bank ID code 1IBL) (1).

1. Ogle JM, et al. (2001) Recognition of cognate transfer RNA by the 30S ribosomal subunit. *Science* 292:897–902.

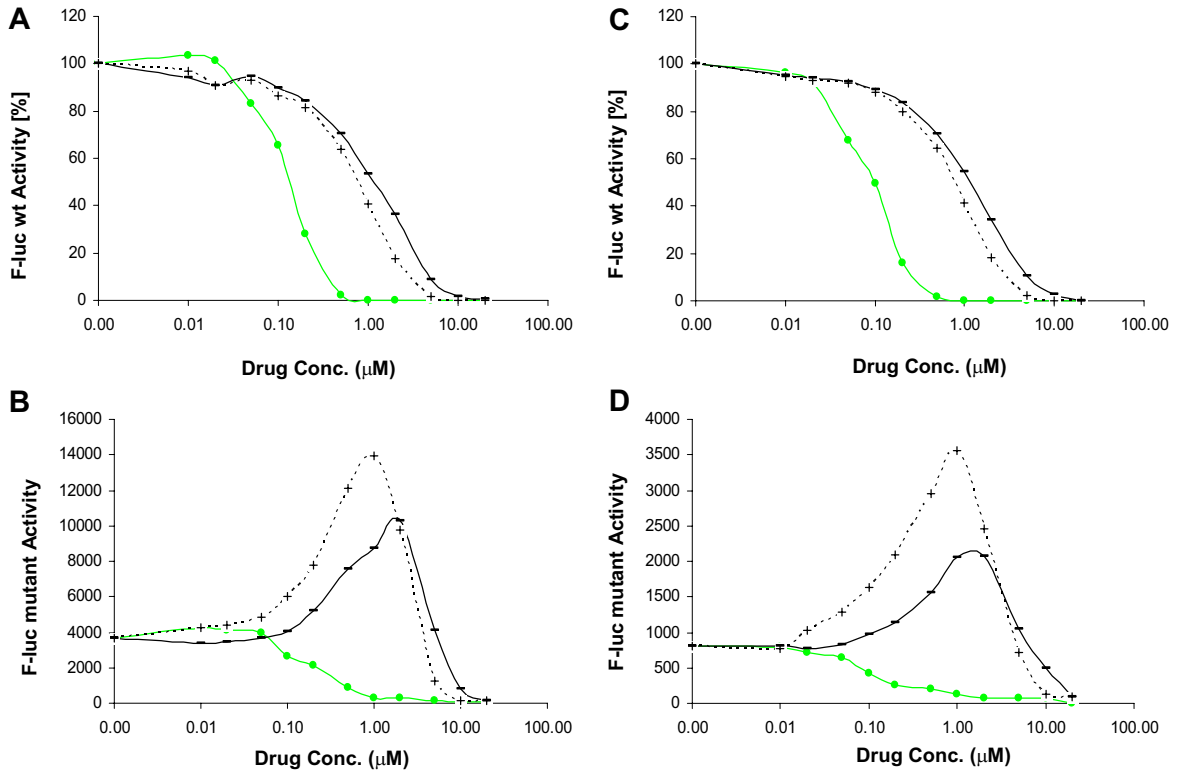

Fig. S3. Apramycin activity on bacterial ribosomes in comparison with aprosamine; neamine was used as control. (*A* and *B*) *E. coli* ribosomes. (*C* and *D*) *M. smegmatis* ribosomes. (*A* and *C*) Translation inhibition as measured by firefly enzymatic activity upon translation of wild-type luc mRNA. (*B* and *D*) Misreading induction as measured by firefly enzymatic activity upon translation of F-luc mRNA 245 CGC mutant. Apramycin, filled green circles and solid green line; aprosamine, dashes and solid black line; neamine, crosses and broken line.

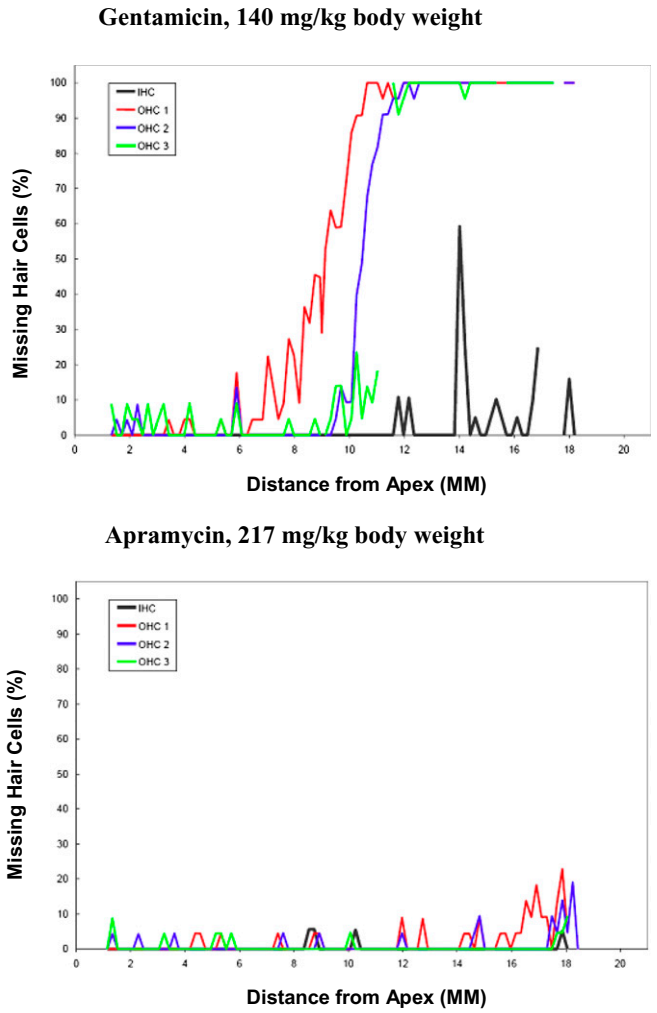

Fig. S4. Cytocochleograms showing quantitative evaluation of hair cell loss. Surface preparations (as shown in Fig. 3 for murine explants) of guinea pig cochleae were evaluated quantitatively by counting the presence or absence of hair cells along the entire length of the cochlea. (*Upper*)After guinea pigs were treated with 140 mg gentamicin/kg body weight, outer hair cells (OHC) in the apex of the cochlea are still well preserved, but loss of cells increases steeply toward the base with a total loss in the lower 50% of the cochlea. Inner hair cells (IHC) are better maintained and show scattered loss toward the base. (*Lower*) In contrast, after treatment with 217 mg apramycin/kg body weight, only minimal loss of cells is observed. Representative examples of treatment with gentamicin and apramycin are shown.

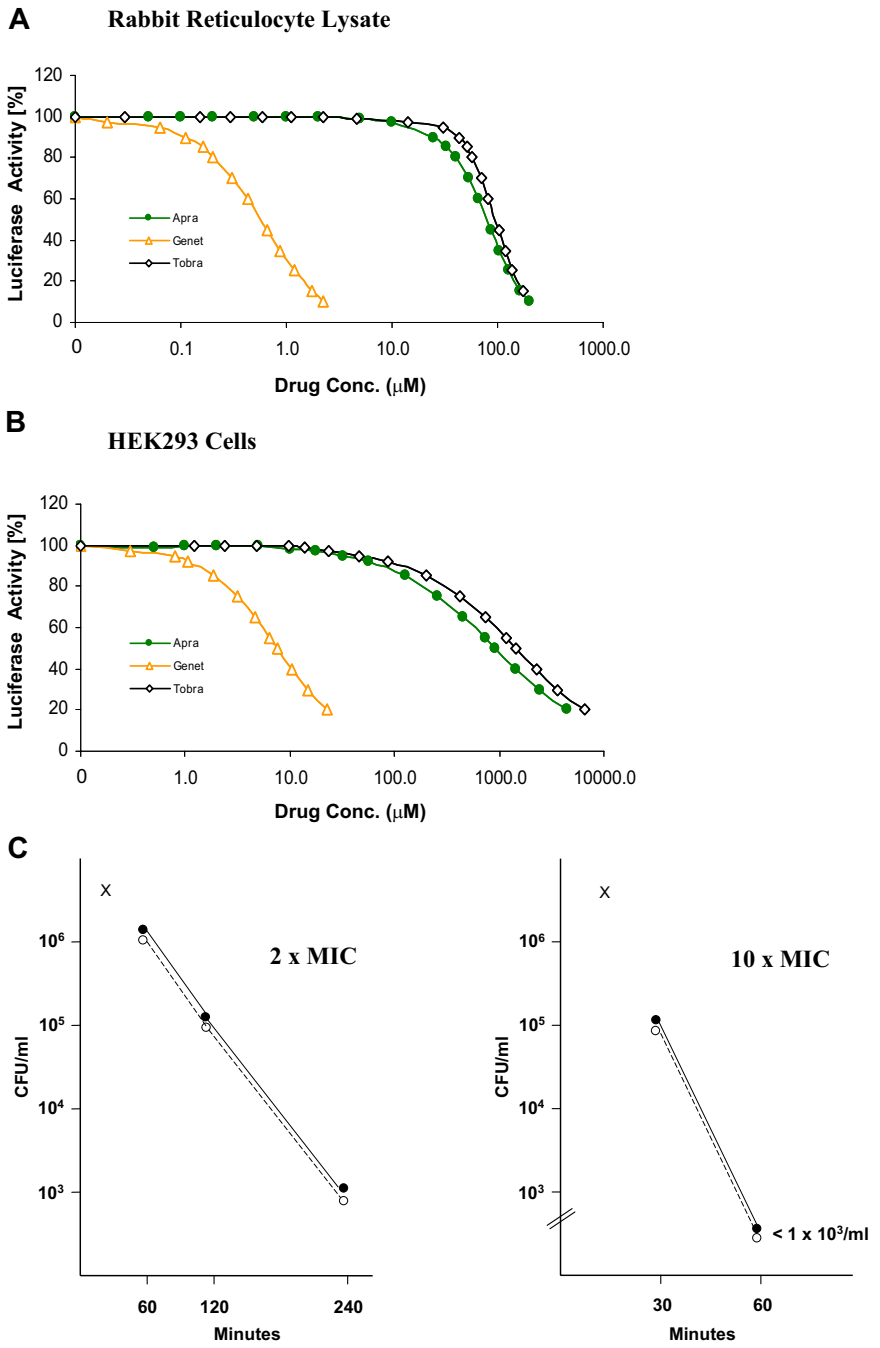

Fig. S5. Apramycin inhibition of eukaryotic cytosolic protein synthesis and apramycin bactericidal activity. (*A*) Aminoglycoside-induced inhibition of eukaryotic cytosolic protein synthesis as assessed by translation of luciferase mRNA in cell-free translation assays using rabbit reticulocyte ribosomes. (*B*) Whole-cell assays using HEK293 cells transfected with a luciferase reporter construct. Geneticin was used as control aminoglycoside with high activity against eukaryotic cytosolic protein synthesis. The IC_{50} ratios of Geneticin:apramycin:tobramycin for rabbit reticulocyte ribosomes are 1:141:167; the corresponding ratios for HEK293 cells are 1:132:183. Apramycin is represented by filled green circles, Geneticin by open orange triangles, and tobramycin by open black rhombi. Data analysis for idealized curves was done with Prism 5 (GraphPad Software Inc.). (*C*) Bactericidal activity of apramycin in comparison with Gentamicin. *E. coli* (5×10^6/mL) was incubated for the indicated times with a drug concentration corresponding to 2× MIC or 10× MIC, and cfu were determined by plating. x = inoculum, filled circle = apramycin, open circle = gentamicin.

Table S1. Activity of apramycin in comparison with available aminoglycosides: Recombinant *E. coli* with defined aminoglycoside-modifying resistance determinants

Strain	Resistance determinant	MIC (mg/L)			
		Apramycin	Gentamicin	Tobramycin	Kanamycin
AG006	—	4	0.5	0.5	1–2
AG007	AAC(3)	8	32–64	4	8
AG008	ANT(2″)	4	16	8–16	16–32
AG009	AAC(6′)	8	8–16	64–128	256
AG036	ANT(4′)	4	0.5	16–32	16–32
AG037	APH(3′)	4	0.25	1–2	>256

Table S2. Activity of apramycin in comparison with available aminoglycosides: clinical isolates of *E. coli, P. aeruginosa*, and methicillin-resistant *S. aureus* (MRSA)

Strain	MIC (mg/L)				
	Apramycin	Gentamicin	Tobramycin	Kanamycin	Amikacin
AG055 *E. coli*	8	16	2	4–8	4
AG056 *E. coli*	8–16	2	2	4–8	4
AG058 *E. coli*	8–16	2–4	2	8	8
AG003 *E. coli*	8–16	128–256	8	16	4
AG059 *E. coli*	8	32–64	32–64	≥256	4
AG060 *E. coli*	8	128	16	≥256	4
AG061 *E. coli*	16	256	16–32	256	8
AG062 *E. coli*	8–16	128–256	128–256	128–256	16–32
AG063 *E. coli*	8	≥256	≥256	≥256	16–32
AG064 *E. coli*	8	128	64–128	64–128	8
AG065 *E. coli*	8	64–128	64	64	8
AG066 *E. coli*	8–16	128–256	128	4–8	8
AG067 *E. coli*	16	128–256	128–256	≥256	16
AG068 *E. coli*	8–16	64–128	32–64	≥256	8
AG077 *P. aeruginosa*	8	2	1	128	4
AG083 *P. aeruginosa*	16	4–8	1–2	256	8
AG084 *P. aeruginosa*	4	32	16–32	>256	32
AG087 *P. aeruginosa*	16	4–8	2	128–256	16
AG041 MRSA	8	0.5	0.5–1	2–4	4–8
AG040 MRSA	8	0.5	≥256	128–256	16–32
AG044 MRSA	16	16	8	64	4
AG045 MRSA	8–16	16	8	64	4
AG053 MRSA	8	64	16–32	256	8–16
AG042 MRSA	8	32–64	≥256	256	16
AG046 MRSA	8–16	≥256	128–256	>256	32
AG047 MRSA	8–16	≥256	≥256	>256	256
AG048 MRSA	8–16	≥256	≥256	>512	256
AG050 MRSA	4–8	128	32–64	>256	16
AG051 MRSA	8	128	32–64	>256	8–16
AG052 MRSA	8	16–32	8–16	>256	16

Table S3. Antimycobacterial activity of apramycin: clinical isolates of *M. tuberculosis*, *M. avium-intracellulare*, and *M. kansasii*

	Apramycin (mg/L)				Amikacin (mg/L)			
Strain	0.25	1	4	10	0.25	1	4	10
176949/08 *M. tuberculosis*	R	S	S	S	R	S	S	S
177581/08 *M. tuberculosis*	R	S	S	S	R	S	S	S
177958/08 *M. tuberculosis*	R	S	S	S	R	S	S	S
178122/08 *M. tuberculosis*	R	S	S	S	S	S	S	S
178242/08 *M. tuberculosis*	R	S	S	S	S	S	S	S
178331/08 *M. tuberculosis*	R	S	S	S	R	S	S	S
178557/08 *M. tuberculosis*	R	S	S	S	R	S	S	S
178594/08 *M. tuberculosis*	R	S	S	S	S	S	S	S
177712/08 *M. tuberculosis*	R	S	S	S	S	S	S	S
177809/08 *M. tuberculosis*	R	S	S	S	S	S	S	S
182034/06 *M. avium-intracellulare*	R	R	S	S	R	R	S	S
182124/07 *M. avium-intracellulare*	R	R	S	S	R	R	S	S
182550/07 *M. avium-intracellulare*	R	R	S	S	R	R	S	S
177227/06 *M. kansasii*	R	R	S	S	R	R	S	S
180235/06 *M. kansasii*	R	R	S	S	R	R	S	S

R, resistant; S, susceptible.

Table S4. Antimycobacterial activity of apramycin: clinical isolates of multidrug-resistant *M. tuberculosis*

	Apramycin (mg/L)			
Strain	0.25	1	4	10
186005/09	R	S	S	S
186010/09	R	S	S	S
186013/09	R	S	S	S
186014/09	R	S	S	S
186002/10	R	S	S	S

R, resistant; S, susceptible.

Table S5. Antimycobacterial activity of apramycin: clinical isolates of *M. abscessus*, *M. massiliense*, and *M. bolletii*

	MIC (mg/L)				
Strain	Apramycin	Gentamicin	Tobramycin	Kanamycin	Amikacin
500039/08 *M. abscessus*	2	16	32	2	4
179363/08 *M. abscessus*	4	32	64	8	16
500042/08 *M. abscessus*	4	16	32	16	16
186139/07 *M. massiliense*	8	32	64	8	16
500044/09 *M. massiliense*	4	8	16	4	4
177217/10 *M. massiliense*	8	32	64	8	16
181739/08 *M. bolletii*	8	32	64	16	32
179693/10 *M. bolletii*	8	32	64	16	32
183177/08 *M. bolletii*	4	32	64	8	32

Table S6. Plasmids used

Plasmid designation	Marker	Genotype
pH128 pMV361Δ*aph-hyg*-1408G	Hyg	A1408G
PZ176 pMV361Δ*aph-hyg*-1491A	Hyg	G1491A
PZ178 pMV361Δ*aph-hyg*-1491C	Hyg	G1491C
PZ177 pMV361Δ*aph-hyg*-1491U	Hyg	G1491U
pH127 pMV361Δ*aph-hyg*-Cyt14	Hyg	Cytosolic hybrid
pH121 pMV361Δ*aph-hyg*-Mit13	Hyg	Mitochondrial hybrid
pH124 pMV361Δ*aph-hyg*-Mit13 A1555G	Hyg	Mitochondrial A1555G hybrid

Table S7. Strains used

M. smegmatis strain	No.	Plasmid used	Genotype
Δ*rrnB rrsA*	SZ380	Wild type	Wild type
Δ*rrnB rrsA*(A1408G)	SZ461	pH128	A1408G
Δ*rrnB rrsA*(G1491A)	SZ463	PZ176	G1491A
Δ*rrnB rrsA*(G1491C)	SZ469	PZ178	G1491C
Δ*rrnB rrsA*(G1491U)	SZ505	PZ177	G1491U
Δ*rrnB rrsA*(Cyt14)	SZ479	pH127	Cytosolic hybrid
Δ*rrnB rrsA*(Mit13)	SZ485	pH121	Mitochondrial hybrid
Δ*rrnB rrsA*(Mit13-A1555G)	SZ496	pH124	Mitochondrial A1555G hybrid

Table S8. Summary of crystallographic data and refinement

Data collection	30S–apramycin complex
Space group	$P4_12_12$
Cell dimensions	
a, *b*, *c* (Å)	*a* = 402.2, *b* = 402.2, *c* = 175.0
α, β, γ (°)	α=β=γ=90
Resolution (Å)	40–3.5 (3.6–3.5)*
Rsym or Rmerge	10.2 (110.2)
I/σ*I*	16.0 (2.0)
Completeness (%)	99.7 (99.5)
Redundancy	6.9 (7.2)
Refinement	
Resolution (Å)	45.0–3.5
No. unique reflections	178,694
*R*work/*R*free	19.4/23.5
No. atoms	
RNA	32,888
Protein	19,239
Ions	221
Ligands	185
B-factors†	
RNA	123.0
Protein	134.0
Ions	97.4
Ligand	109.5
R.m.s. deviations	
Bond lengths (Å)	0.0068
Bond angles (°)	1.203

*Highest resolution shell is shown in parentheses.
†Average B-factors were calculated from the model after grouped isotropic B-factor refinement of CNS.